Curr Genet (2004) 44: 317–328
DOI 10.1007/s00294-003-0439-7

RESEARCH ARTICLE

Alexandra L. Grishchuk · Rolf Kraehenbuehl
Monika Molnar · Oliver Fleck · Juerg Kohli

Genetic and cytological characterization of the RecA-homologous proteins Rad51 and Dmc1 of *Schizosaccharomyces pombe*

Received: 2 June 2003 / Revised: 27 July 2003 / Accepted: 29 July 2003 / Published online: 29 August 2003

Abstract The *Schizosaccharomyces pombe rad51*$^+$ and *dmc1*$^+$ genes code for homologues of the *Escherichia coli* recombination protein RecA. Deletion of *rad51*$^+$ causes slow growth, retardation of cell division and a decrease in viability. *rad51*Δ cells have a defect in mating-type switching. The DNA modification at the mating-type locus required for mating-type switching contributes to slow growth in the *rad51* mutant. Cell mating is reduced in crosses homozygous for *rad51*Δ. Ectopic expression of the *dmc1*$^+$ gene allowed us to demonstrate that the reduction in meiotic recombination in *dmc1* mutants is not caused by a disturbance of *rad24* expression from the *dmc1-rad24* bicistronic RNA. We describe the functional defects of terminally epitope-tagged Dmc1 and Rad51 and discuss it in terms of protein interaction. Presumptive Rad51 and Dmc1 foci were detected on spreads of meiotic chromatin.

Keywords Rad51 · Dmc1 · Slow growth · Meiotic recombination

Introduction

Homologous recombination maintains the integrity of the genome through accurate repair of DNA damage and confers genetic diversity. Homologous recombination in bacteria involves the RecA protein along with other factors (for reviews, see Kowalczykowski et al. 1994; Smith et al. 1995). Mutation of *recA* completely abolishes conjugational recombination and DNA damage-induced recombinational repair. Biochemical studies revealed that the RecA protein catalyzes the invasion of single-stranded DNA into homologous duplex DNA.

Homologues of RecA have been identified in a wide range of organisms, including plants, flies and vertebrates (Bezzubova et al. 1993; Shinohara et al. 1993; Akaboshi et al. 1994; Doutriaux et al. 1998). Usually, the genomes of eukaryotic organisms have several proteins related to bacterial RecA. *Saccharomyces cerevisiae* has four *recA*-like genes: *RAD51*, *RAD55*, *RAD57* and *DMC1* (Aboussekhra et al. 1992; Basile et al. 1992; Bishop et al. 1992; Shinohara et al. 1992; Story et al. 1993; Donovan et al. 1994; Hays et al. 1995). Budding yeast *rad51* mutants are viable, but highly sensitive to DNA-damaging agents, such as ionizing radiation and methylmethane sulfonate (MMS). In contrast, mouse *RAD51*$^{-/-}$ knockouts are embryonic lethal, indicating an essential role for Rad51 early in development (Lim and Hasty 1996; Tsuzuki et al. 1996). During meiosis, yeast *rad51* mutants accumulate double-strand breaks (DSBs), thus manifesting defects in the formation of downstream recombination intermediates; and they show decreased viability during sporulation and other meiosis defects (Shinohara et al. 1992; Rockmill et al. 1995). Immunofluorescence staining of nuclear spreads from *Sac. cerevisiae* (Shinohara et al. 1992) and human and mouse spermatocytes (Barlow et al. 1997) revealed that Rad51 localizes to distinct nuclear foci during meiotic prophase. Several biochemical properties of Rad51 protein, especially the ability to promote homologous pairing and strand transfer, resemble those of RecA (Sung 1994; Baumann et al. 1996). Rad51 was defined as the primary RecA homologue in eukaryotes.

Dmc1 of *Sac. cerevisiae* is expressed only during meiosis and is required for normal recombination and meiosis progression (Bishop et al. 1992). Plant and mammal *dmc1*$^{-/-}$ mutants are viable, but infertile (Pittman et al. 1998; Couteau et al. 1999). Meiotic DSBs in the *dmc1* mutant cannot be processed. Like

Communicated by M. Yamamoto

A. L. Grishchuk · R. Kraehenbuehl · M. Molnar
O. Fleck · J. Kohli (✉)
Institute of Cell Biology, University of Bern,
Baltzerstrasse 4, 3012 Bern, Switzerland
E-mail: juerg.kohli@izb.unibe.ch
Tel.: +41-31-6314654
Fax: +41-31-6314616

Rad51, Dmc1 is required for synapsis of homologous chromosomes (Bishop et al. 1992). It forms foci during meiotic prophase that co-localize with Rad51 foci (Bishop 1994). Besides these similarities, Rad51 and Dmc1 proteins also show differences, which led to the proposal that they have both overlapping and distinct roles in meiosis (Dresser et al. 1997; Shinohara et al. 1997). Interestingly, no Dmc1 homologue was found in *Drosophila melanogaster* or *Caenorhabditis elegans* (for a review, see Masson and West 2001).

In *Schizosaccharomyces pombe*, homologues of Rad51 (also called Rhp51) and Dmc1 have been identified (Muris et al. 1993; Jang et al. 1994; Fukushima et al. 2000), as well as three additional RecA-like proteins: Rhp55, Rhp57 and Rlp1 (Khasanov et al. 1999; Tsutsui et al. 2000; V.I. Bashkirov 2000, personal communication). Similar to budding yeast, *Sch. pombe rad51* mutants are highly sensitive to DNA lesions resulting from exposure to MMS, γ- or UV-irradiation (Muris et al. 1993; Park et al. 1998). *rad51* deletion strains show a reduction in mitotic homologous DNA integration, meiotic recombination and spore viability (Muris et al. 1997; Khasanov et al. 1999). *Sch. pombe rad51* mutant strains grow slowly and show aberrant cell morphology which is not observed in *Sac. cerevisiae* (Muris et al. 1993; Jang et al. 1995).

Some properties of a *Sch. pombe dmc1* mutant were described by Fukushima et al. (2000). This mutant displays no defects during vegetative growth; and *dmc1*$^+$ is expressed exclusively during meiosis. In contrast to mammalian and some budding yeast mutants that arrest in meiosis, the *Sch. pombe dmc1* mutant is proficient in meiosis and spore formation. Intergenic and intragenic recombination is reduced in *dmc1*$^{-/-}$ crosses.

Most published studies on *rad51* and *dmc1* were done with strains carrying incomplete gene disruptions. We constructed and analyzed strains with full deletions of the open reading frames (ORFs) of *rad51* and *dmc1*. We studied the transcription of *rad51*$^+$ and *dmc1*$^+$ during meiosis and a possible interaction of *dmc1*$^+$ and *rad24*$^+$ expression. The *rad51* phenotypes in slow growth and cell mating were characterized in detail. N- and C-terminal epitope-tagging of Dmc1 and, very probably, C-terminal tagging of Rad51 resulted in loss-of-function phenotypes. The observations made with several constructions are discussed in terms of protein interactions. The cytological localization of Rad51 and tagged Dmc1 proteins during meiosis is described.

Materials and methods

Strains, media and growth conditions

The genotypes of *Sch. pombe* strains used in this study are listed in Table 1. *Escherichia coli* strain DH5α was used for plasmid isolation. The standard *Sch. pombe* media yeast extract agar (YEA) and liquid (YEL), malt extract agar (MEA), minimal medium (MMA) and the general genetic methods were as described by Gutz et al. (1974). When necessary, 0.01% supplements was added to the media. For meiotic time-course experiments, the synthetic minimal medium PM (Beach et al. 1985) and PM without NH_4Cl (Watanabe et al. 1988) were used. Growth of *Sch. pombe* strains and meiotic time-courses were performed at 30 °C. Crosses and growth of cells for mating-type analysis were performed at 25 °C. Growth of cells for pedigree analysis was at 30 °C in YEL cultures and at 25 °C on YEA plates. Iodine staining of colonies was as described by Leupold (1955).

Construction of the *rad51* and *dmc1* deletion strains

Complete deletion of the *rad51* gene was obtained by replacement of the coding region of *rad51* with the *his3*$^+$ marker gene. The prad51 plasmid (a kind gift from A. Shinohara) derives from pUC118, which contains the 4.4-kb *Bam*HI genomic fragment from the *rad51* locus. This plasmid was used for PCR to amplify 473 bp of the upstream flanking sequence of *rad51* and 432 bp of the downstream flanking sequence of *rad51*. In the upstream flanking sequence, *Not*I and *Spe*I restriction sites were introduced by PCR at the 5′ and 3′ ends, respectively. In the downstream flanking

Table 1 *Schizosaccharomyces pombe* strains used in this study

Strain	Genotype	
968	h^{90}	
975	h^+	
1-25	h^+	*ade6-M216*
3-106	h^-	*lys7-1*
4-150	h^+	*lys7-2*
77-3045	h^+	*rad51::his3 his3-D1 mat1ΔP17::LEU2 leu1-32 arg6-1*
88–3484	h^-	*rad51::his3 his3-D1 ade7-152 smt0*
89-3536	h^-	*ade6-M216 smt0*
89-3537	h^+	*ade6-M210 mat1ΔP17::LEU2 leu1-32*
AG44	h^+	*dmc1-C3HA lys7-2*
AG47	h^-	*dmc1-C3HA lys7-1*
AG53	h^-	*dmc1::ura4 lys7-1 ura4-D18*
AG56	h^+	*dmc1::ura4 lys7-2 ura4-D18*
AG58	h^+	*dmc1::ura4 ura4-D18 ade6-M216*
AG66	h^-	*rad51::his3 his3-D1 ade6-M216 smt0-0*
AG69	h^+	*rad51::his3 his3-D1*
AG70	h^+	*rad51::his3 his3-D1 mat1ΔP17::LEU2 leu1-32*
AG72	h^+	*rad51::his3 his3-D1 ade6-M210 mat1ΔP17::LEU2 leu1-32*
AG84	h^-	*dmc1::ura4 leu1-32 ura4-D18*
AG100	h^-	*dmc1-CGFP lys7-1*
AG101	h^+	*dmc1-CGFP lys7-2*
AG104	h^-	*dmc1*$^+$ *dmc1::ura4 lys7-1 ura4-D18*
AG105	h^+	*dmc1*$^+$ *dmc1::ura4 lys7-2 ura4-D18*
AG302, AG304	h^-	*dmc1-N3HA lys7-1*
AG303, AG305	h^+	*dmc1-N3HA lys7-2*
AG306, AG308	h^-	*dmc1-NMyc lys7-1*
AG307, AG309	h^+	*dmc1-NMyc lys7-2*
AG310, AG312	h^-	*dmc1-NGFP lys7-1*
AG311, AG313	h^+	*dmc1-NGFP lys7-2*
AG484	h^+	*rad51-CGFP ade6-M216*
AG485	h^+	*rad51-CMyc ade6-M216*
AG491	h^{90}	*rad51::his3 his3-D1*
RK1	h^-	*his3-D1 smt0*
RK2	h^-	*ura4-D18 smt0*
RK3	h^-	*smt0 ade7-152*
RK4	h^+	*mat1ΔP17::LEU2 leu1-32 arg6-1*
D1	h^-/h^+	*ade6-M210/ade6-M216*
D2	h^-/h^+	*ade6-M210/ade6-M216 dmc1-CGFP/dmc1-CGFP*
D3	h^-/h^+	*ade6-M210/ade6-M216 dmc1-C3HA/dmc1-C3HA*

sequence, *Sal*I and *Asp*718 restriction sites were introduced at the 5′ and 3′ ends, respectively. The PCR fragments were then integrated into the pKLG-497 plasmid, a derivative of pBluescript SK(−) containing a 2-kb fragment carrying the *his3*$^+$ marker gene (Burke and Gould 1994). The resulting gene disruption plasmid was named pRK2. A 2.9-kb *Not*I/*Asp*718 fragment from pRK2, carrying the *his3*$^+$ marker gene with *rad51*-specific flanking sequences, was used to transform strain RK1 (*h*$^-$ *smt0 his3-D1*) by the lithium acetate method (Ito et al. 1983). Proper integration of the fragment into the genome was verified by Southern blot analysis. Full deletion of the *dmc1* gene was obtained by replacement of the coding region of *dmc1* with the *ura4*$^+$ marker gene. The pdmc1 plasmid (a kind gift from A. Shinohara) derives from pBluescript KS(+), which contains the 3.6-kb *Xba*I/*Hin*dIII genomic fragment from the *dmc1* locus. This plasmid was used for PCR to amplify 585 bp of the upstream flanking sequence and 484 bp of the downstream flanking sequence of *dmc1*. In the upstream flanking sequence, *Asp*718 and *Sal*I restriction sites were introduced by PCR at the 5′ and 3′ ends, respectively. In the downstream flanking sequence, *Pst*I and *Not*I restriction sites were introduced at the 5′ and 3′ ends, respectively. The PCR fragments were then integrated into pB4-2 plasmid, a pBluescript SK(−) plasmid containing the 1.8-kb *Hin*dIII fragment carrying the *ura4*$^+$ marker gene (Grimm et al. 1988), to yield the gene disruption plasmid pRK1. A 2.8-kb *Asp*718/*Not*I fragment carrying the *ura4*$^+$ marker gene with *dmc1*-specific flanking sequences from pRK1 was used to transform strain RK2 (*h*$^-$ *smt0 ura4-D18*). Proper integration of the fragment into the genome was verified by Southern blot analysis.

Pedigree analysis, determination of mating efficiency and UV-sensitivity tests

For pedigree analysis, cells in the logarithmic phase of growth were spatially separated on YEA plates and incubated for 8–10 h. Subsequently, the number of progeny cells was scored for each inoculated cell. Cells that did not divide at least once during 16 h of incubation were considered dead. For determination of mating efficiency, cells of opposite mating type were crossed on MEA at 25 °C. After 3 days, the number of vegetative cells (C), zygotes (Z), asci (A) and spores (S) was scored microscopically. A minimum of a total of 300 units were counted in each cross and 7–13 crosses were performed for each mutant. The mating efficiency was calculated as $(A+Z+0.25S)/(A+Z+0.25S+0.5C)\times 100\%$. UV sensitivity was tested by drop assay. Cells were grown in YEL to stationary phase, spotted in different dilutions onto YEA plates and irradiated in a UV Stratalinker (Stratagene). Plates were incubated for 3 days at 30 °C. The test was repeated at least once.

Meiotic time-course experiments including cytology

Induction of meiosis and 4′,6-diamino-2-phenylindole (DAPI) staining of DNA and immuno-staining of spreads were as described by Parisi et al. (1999) with the following alterations: instead of Novozym, lysing enzyme (1.5 mg/ml; Sigma L-2265) was used, no overnight blocking was performed, blocking buffer for 15 min blocking was not diluted and washes of slides were extended to 15 min in PBS with 0.1% Photo-Flo (Kodak) and twice for 15 min in PBS with 0.05% Triton X-100. The following primary antibodies were used: purified rabbit anti-GFP IgG diluted 1:500 to 1:1,000 (Seedorf et al. 1999), purified rabbit anti-human Rad51 IgG diluted 1:100 to 1:200 (sc-8349; Santa Cruz Biotechnology) and guinea pig anti-*Sac. cerevisiae* Rad51 serum (described by Shinohara et al. 2000). The secondary antibodies used were: purified goat anti-rabbit IgG conjugated with Alexa Fluor 488 diluted 1:500 (A-11008; Molecular Probes) and purified goat anti-guinea pig IgG conjugated with Alexa Fluor 555 diluted 1:500 (A-21435; Molecular Probes). Nuclear spreads were observed with a Nikon eclipse E600 fluorescence microscope. Images were taken with a Nikon DXM1200 polychrome digital camera.

Total RNA was prepared from 50-ml aliquots of time-course culture as described by Grimm et al. (1991). mRNA was separated from 500 μg of total RNA using an Oligotex poly(A)$^+$ mRNA isolation kit (Quiagen). To facilitate the precipitation of mRNA, about 50 μg of tRNA was added to each sample. Hybridization with a ^{32}P-labeled *rad51*, *dmc1* or *byr1* (Nadin-Davis and Nasim 1990) probe was performed by the formamide hybridization protocol, as specified by the manufacturer (Bio-Rad). The *rad51* probe was a 0.2-kb PCR fragment from positions −1 to 216 in the ORF corresponding to the N-terminal part of the protein, where the homology with other RecA-like proteins is lowest. The *dmc1* probe was a 0.5-kb PCR fragment from positions 380 to 871 in the ORF. The *byr1* probe (a kind gift from A.M. Schweingruber) was a 0.4-kb PCR fragment from positions 976 to 1,387 in the ORF.

Spore viability and meiotic recombination

Spore viability was determined by tetrad and random spore analysis. Random spores from 5–15 independent crosses were counted under the microscope and appropriate amounts plated onto YEA. For intergenic recombination analysis, spore colonies were randomly picked (135–224 in each cross), grown on YEA master plates and then replicated onto MMA with appropriate supplements. For intragenic recombination analysis, the number of prototrophic spore colonies was counted on selective MMA and normalized to the amount of viable spores.

Construction of diploids

Parental strains carrying *ade6-M210* or *ade6-M216* and *smt0* or *mat1P*Δ*17::LEU2* mutations were crossed on supplemented MEA plates: strains 89-3536 and 89-3537 to obtain a wild type diploid and strains AG66 and AG72 to obtain a *rad51*Δ diploid. The next day, some material from the plates was diluted and plated onto selective MMA plates. Under these conditions, zygotes not yet committed to meiosis returned to vegetative growth. Due to interallelic complementation between the mutations *M210* and *M216*, only these diploid cells were able to form adenine-independent colonies on MMA, which were large and white. Microcolonies growing on MMA were avoided. Spontaneous chromosome III loss in *M210*/*M216* diploids led to adenine dependence and the formation of red sectors in white colonies. The diploids used in the cytological experiments were not carrying *smt0* or *mat1P*Δ*17::LEU2* mutations.

Ectopic expression of the *dmc1*$^+$ gene

To introduce a wild-type *dmc1*$^+$ gene into a *dmc1::ura4*$^+$ strain at the ectopic *leu1* locus, we constructed plasmid pJKdmc1, carrying the *leu1*$^+$ and *dmc1*$^+$ genes. A 2.9-kb *Xba*I/*Hpa*I fragment from the pdmc1 plasmid was introduced into pJK148 (Keeney and Boeke 1994) and digested with *Xba*I and *Hin*cII. The resulting plasmid was linearized with *Bsu*36I, which cuts in *leu1*$^+$, and transformed into strain AG84 (*h*$^-$ *dmc1::ura4*$^+$ *ura4-D18 leu1-32*). Genomic DNA of *leu*$^+$ transformants was analyzed by Southern blot hybridization to identify a strain with a single integration at the *leu1* locus. The *leu1* probe used for hybridization was a ^{32}P-labeled 0.9-kb PCR fragment derived from positions 68 to 939 of the ORF.

Fusion of epitope tags to *dmc1*$^+$ and *rad51*$^+$ and C-terminal tagging

To fuse 3HA, 13Myc or GFP epitope tags to *dmc1*$^+$ and *rad51*$^+$ genes, we used the PCR-based gene-targeting method described by Bahler et al. (1998). The hybrid primers contain 100 nt identical to the target loci at their 5′ ends and 20 nt identical to pFA6akanMX6-based plasmids at their 3′ ends. In case of *dmc1*$^+$ tagging, the 100-nt stretches were from position 971 to 1,070 and from 1,173 to 1,074, relative to the translation start codon. In case of the *rad51*$^+$ tagging, the 100-nt stretches were from position 996 to 1,095 and from 1,326 to 1,226, relative to the translation start codon. The PCR reactions with these primers yielded fragments containing the epitope tag, the *kanMX6* marker and 100 bp of sequence homologous to the target locus on each side. These fragments were used to transform strains 89-3537 or 1-25. Transformants with integration of *kanMX6* were selected on YEA plates containing 100 mg G418/l. PCR analysis using a primer specific for the *kanMX6* sequence and another specific for *dmc1* or *rad51* allowed the identification of transformants with integrations at the *dmc1* and *rad51* target loci. The integrations at the *dmc1* locus resulted in the deletion of the *dmc1* stop codon only. In this way, the region downstream of *dmc1* remained unchanged. This may prevent interference with expression of the *rad24* gene located 0.8 kb downstream of *dmc1*. At the *rad51* locus, 130 nt including the stop codon and downstream sequence were deleted.

N-terminal tagging

For an overview of N-terminal tagging, see Fig. 1.

To fuse 3HA, 13Myc or GFP epitope tags to the *dmc1*$^+$ gene, we constructed a set of plasmids, pdmc1-N(tag), by fusion PCR. The untranslated region upstream of the *dmc1*$^+$ ORF was amplified from pdmc1 using primers S0025 (5′-AAATTGAACGAGTCTTTTGC-3′) and S0026 (5′-*GTTAATTAACCCGGGGATCCG*CATTGCACTTTATTTTTATATTGAACG-3′), where the sequence from pFA6a-kanMX6-based plasmids (Bahler et al. 1998) is in italics. The N-terminal region of the *dmc1*$^+$ ORF was amplified from pdmc1 using one of the primers S0037, S0039 or S0038 and S0034 (5′-CATATCTCGAGGAAGCTGGG-3′). Primers S0037, S0039 and S0038 contained at their 5′ ends the following tag-specific sequences: CAGATTACGCTGCTCAGTGC for the 3HA tag (S0037), CAATCACGAGGGAATTCGCGCC for the 13Myc tag (S0039) and CACATGGCATGGATGAACTATAC for the GFP tag (S0038). The tag-specific sequences were followed by 5′-*GGAGGAGGAGGA*TGGAAGAATTCGCAGAGGGG-3′. A sequence coding for four glycine residues is in italics; and the rest is specific to the 3′ end of the *dmc1* ORF. The four glycines were inserted to increase the probability of protein-folding into two independent domains. The epitope tag sequences were amplified from plasmids pFA6a-3HA-kanMX, pFA6a-13Myc-kanMX or pFA6a-GFP-kanMX, using primer S0027 (5′-CGGATCCCCGGGTTAATTAAC-3′) together with one of the following: S0028 (5′-GCACTGAGCAGCGTAATCTG-3′) for the 3HA tag, S0035 (5′-GGCGCGAATTCCCTCGTGATTG-3′) for the 13Myc tag or S0030 (5′-GTATAGTTCATCCATGCCATGTG-3′) for the GFP tag. The PCR products of the untranslated region upstream of the *dmc1*$^+$ ORF and the tag-specific sequences were then fused, using primer S0025 together with one of the following: S0028 (for the 3HA tag), S0035 (for the 13Myc tag) or S0030 (for the GFP tag). The PCR products obtained from the fusion reactions and the 5′ region of the *dmc1*$^+$ ORF were then fused using primers S0025 and S0034. The PCR products obtained from the second fusion were digested with *Afl*II and *Bsa*BI and integrated into the pdmc1 plasmid digested with *Afl*II and *Bsa*BI, to yield the plasmids pdmc1-N(3HA), pdmc1-N(13Myc) and pdmc1-N(GFP). Each plasmid was then digested with *Xba*I and *Eco*47III, yielding fragments containing the coding sequence of the tagged *dmc1* gene flanked by 1.6 kb of the 5′ flanking region and 0.8 kb of the 3′ flanking region (Fig. 1). These fragments were used to transform strain AG58. Ura$^-$ transformants were selected on YEA plates containing fluoroorotic acid (1 g/l) and checked for correct integration by PCR, using primers S0040 (5′-TCTCCAGATATGCCTGAAGC-3′) and S0041 (5′-CGATGTTTTACAGGAAGCCC-3′). The presence of the epitope tags in the transformed strains was confirmed by PCR, using primers S0042 (5′-CAGACAGTATTGGTTCAACC-3′; located upstream of S0025) and S0034 (see above).

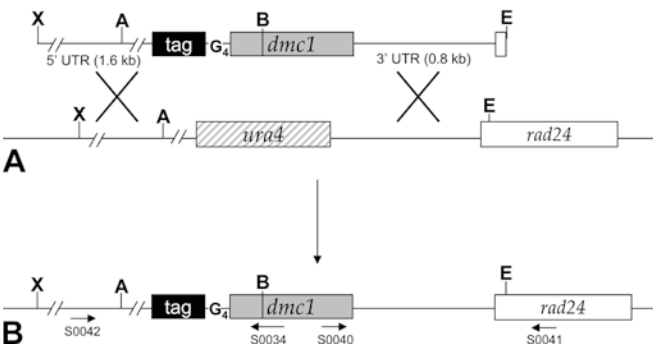

Fig. 1A, B Schematic diagram of N-terminal tagging of the *dmc1*$^+$ gene. **A** *Xba*I/*Eco*47III fragments from pdmc1-N (*tag*) plasmids were used to transform the AG58 strain. **B** Schematic map of the genomic DNA at the *dmc1* locus after transformation. *The boxes* indicate the *dmc1*$^+$ ORF (*gray*), the epitope tag (*black*), the *ura4*$^+$ ORF (*hatched*) and the *rad24*$^+$ ORF (*white*). G_4 indicates a stretch of four glycine residues. Primers used to control for correct integration, and the presence of the tags, are *indicated with arrows*. Restriction sites: *A Afl*II, *B Bsa*BI, *E Eco*47III, *X Xba*I

Results

The phenotypes of the *rad51* and *dmc1* full-gene deletion strains during vegetative growth

The deletions of the *Sch. pombe* genes *rad51* and *dmc1* were constructed as described in the Materials and methods. Mating-type switching in *Sch. pombe* is initiated by a specific DNA modification, probably a single-strand break, at the *mat1* locus (Arcangioli 1998; Dalgaard and Klar 1999). It was proposed that this break is converted to a DSB by DNA replication and that the DSB is repaired by homologous recombination (Arcangioli 1998; Arcangioli and de Lahondes 2000). *smt0* and *mat1PΔ17::LEU2* mutations abolish formation of a DSB at *mat1* (Arcangioli and Klar 1991; Styrkarsdottir et al. 1993). To be able to separate a possible involvement of Rad51 in specific DSB repair at the *mat1* locus from its other roles, we studied *rad51::his3*$^+$ in combination with the *smt0* and *mat1PΔ17::LEU2* mutations. We confirmed the sensitivity of *rad51::his3*$^+$ carrying the *smt0* mutation to UV irradiation and to the alkylating agent MMS in qualitative drop assays (data not shown). This result is consistent with previous observations on incomplete *rad51* gene disruption (Muris et al. 1993; Jang et al. 1995) and with results obtained by Hartsuiker et al. (2001) in a quantitative assay. *rad51*$^-$ cells were previously shown to grow more slowly than the wild type in liquid cultures (Jang et al. 1995). The mutant cells were also larger than the wild type. Slow growth may derive from an extended cell cycle length. To determine whether slow growth of the *rad51* mutant is caused only by extension of the cell cycle or also by decreased viability, we performed a pedigree analysis of *rad51::his3*$^+$ cells using a micromanipulator (see Materials and methods). Compared

Table 2 Pedigree analysis. The standard errors of the means are based on 3–9 experiments, analyzing 10–12 starter cells in each experiment. *Cell viability* Calculated as the number of living cells (cells which divided at least once during the incubation time) divided by the total number of cells scored. *Progeny cells* Average number of cells that arose from a single viable cell after 8–10 h of incubation. *Doubling time* Calculated for viable cells with the assumption that cells were incubated for 9 h

Strain	Cell viability (%)	Progeny cells	Doubling time (min)
Wild type (975)	100 ± 0	8.1 ± 0.1	179 ± 1
rad51 (AG69)	67 ± 3.3	3.1 ± 0.05	331 ± 5
rad51 mat1PΔ17 (AG70)	85 ± 1.9	3.6 ± 0.2	298 ± 16

with the wild type, the average doubling time of *rad51::his3*$^+$ cells was increased and the viability of *rad51::his3*$^+$ cells was decreased (Table 2). Thus, slow growth of the *rad51* mutant is a combined phenotype, caused both by cell cycle elongation and by decreased viability. *rad51::his3*$^+$ cells with no DSB at the mating-type locus (*mat1PΔ17::LEU2*) had better survival than *rad51::his3*$^+$ cells with a wild-type *mat1* locus (Table 2). Therefore, we propose the involvement of *rad51*$^+$ in recombinational repair of the DSB at the mating-type locus.

To study the involvement of *rad51*$^+$ in mating-type switching, we isolated a *h*^{90} *rad51Δ* segregant (AG491) from a *h*$^+$ strain (AG69). In the *h*$^{+N}$ strains, rare recombination events led to reversion to the *h*^{90} configuration at the mating-type locus (Beach and Klar 1984). When restreaked and stained with iodine vapor, this segregant gave rise to mainly iodine-negative colonies and a few mottled colonies, which is in sharp contrast to a *h*^{90} *rad51*$^+$ strain (968), which produces mostly iodine-positive colonies (data not shown). Approximately two-thirds of the iodine-negative colonies were *h*$^-$ and one third was *h*$^+$ (273 iodine-negative colonies of 11 independent restreakings were tested). The vast majority of the *h*$^-$ colonies were stable, not giving rise to mottled or *h*$^+$ colonies (24 *h*$^-$ colonies of four independent origins were tested). These data indicate that *rad51*$^+$ is required for mating-type switching. We also analyzed the mating efficiency of *rad51*$^-$ cells and found that it was reduced approximately 2-fold compared with wild-type cells (Table 3).

In contrast to the *rad51* mutant, *dmc1* deletion strains were not expected to show defects during vegetative growth, based on the results obtained with an insertion of the *ura4*$^+$ gene into the ORF of *dmc1* (Fukushima et al. 2000). Our *dmc1::ura4*$^+$ strains grew normally and showed no sensitivity to UV and MMS (data not shown).

rad51$^+$ and *dmc1*$^+$ expression is induced during meiosis

We performed a synchronized meiotic time-course study of wild-type diploid cells (D1) and analyzed the mRNA from these cells for the presence of *rad51*- and *dmc1*-specific transcripts. The results of this experiment (Fig. 2A) revealed that *rad51*$^+$ was expressed both in vegetatively growing cells before entering meiosis (at time point 0 h) and throughout meiosis (2–10 h) with a peak around 6 h. Several mRNA species were detected in a size range of ~1.0–1.7 kb, which is consistent with the observations of Muris et al. (1993). Some of the bands may also represent cross-hybridization with transcripts of other *recA* like genes: *rhp55*$^+$, *rhp57*$^+$ and *rlp1*$^+$ (see Discussion). *dmc1*$^+$ was expressed specifically during meiosis (4–10 h). The size of a *dmc1*-specific transcript (~2.8 kb) is consistent with the observation of Fukushima et al. (2000).

To bring the transcription of *rad51*$^+$ and *dmc1*$^+$ into the context of the classic landmarks of fission yeast meiosis, we determined different cytological stages during the time-course by staining the cells with DAPI (Fig. 2B). The large number of cells with more than one nucleus 1 h after induction represented the final mitotic division before cells entered the meiotic prophase. The increase of cells with more than one nucleus after ~9 h indicated the onset of meiotic division. Cells with elongated nuclei (horse-tails) are characteristic of prophase I

Table 3 Mating efficiency, meiotic intergenic recombination and spore viability of the *rad51* mutant and other strains with deletions of *rad51* paralogues. Genetic distance (*d*) was calculated as $d = -50\ln\{1-2[R/(R+P)]\}$, where *R* is the number of recombinant colonies and *P* is the number of parental colonies. *ND* Not determined

Strain	Mating efficiency (mean ± SE)	*X*-fold reduction (compared with wild type)	Spore viability (mean ± SE)	*X*-fold reduction (compared with wild type)	Genetic distance ade7–arg6 (mean ± SE)	*X*-fold reduction (compared with wild type)
Wild type (*smt0*)	ND	ND	77.9 ± 7.1	1	13.4 ± 1.4	1
Wild type[a]	25.5 ± 2	1	84 ± 9.1	1	ND	ND
rad51 (*smt0*)	ND	ND	8.6 ± 1.5	9	5.9 ± 2.1	2.3
rad51[a]	11.8 ± 1.3	2.2	2.9 ± 0.3	29	ND	ND
dmc1[a]	36.1 ± 3.7	0.7	75.9 ± 3.8	1.1	ND	ND
rhp55[a]	13.5 ± 2.2	2.3	28.5 ± 3	2.8	ND	ND
rhp57[a]	11.1 ± 2.4	1.9	29.8 ± 4.1	2.9	ND	ND
rlp1[a]	22 ± 3.2	1.2	72.4 ± 4.3	1.2	ND	ND

[a] Spore viability data for these strains are cited from Grishchuk and Kohli (2003), who also describe the strain genotypes

and were observed between 5 h and 10 h. The highest levels of *dmc1*$^+$ and *rad51*$^+$ mRNA at 6–8 h coincided with prophase I, when meiotic recombination occurs.

Deletion of *rad51* affects diploid stability and meiotic phenotypes

To measure meiotic recombination frequency in the *rad51* deletion, we performed crosses homozygous for *rad51::his3*$^+$ and *smt* mutations (88-3484×77-3045). The intergenic recombination frequency between the markers *ade7-152* and *arg6-1* located on the left arm of chromosome II was reduced 2.3-fold compared with the wild type (RK3×RK4) (Table 3). The viability of *rad51::his3*$^+$ spores determined by random spore analysis in the same crosses was 8.6% ± 3.4% (Table 3).

Several attempts to construct a stable diploid homozygous for the *rad51::his3*$^+$ deletion were unsuccessful. We mated *rad51::his3*$^+$ haploid parentals AG66 and AG72. They carry either the *smt0*, or the *mat1P-Δ17::LEU2* mutations. Heterozygosity for *ade6-M210* and *ade6-M216* allowed for selection of diploids on minimal medium due to intragenic complementation. Colonies grew slowly, compared with *rad51*$^+$ diploids. In most cases they contained red sectors, indicating haploidization for chromosome III. The white (diploid) colonies were checked for sporulation following a shift to minimal medium lacking nitrogen. While *rad51*$^+$ diploids efficiently sporulated and formed asci, *rad51::his3*$^+$ diploids formed only a few, abnormally shaped asci. In addition, many cells with abnormal morphology (large branched cells) and dead cells were observed (data not shown). We conclude that diploids homozygous for the deletion of the *rad51* gene are unstable and do not sporulate efficiently.

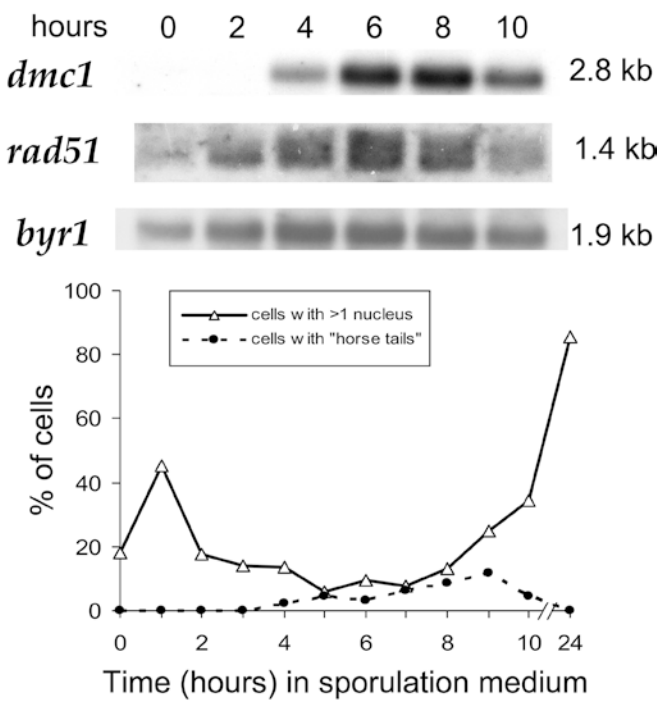

Fig. 2 *dmc1* and *rad51* RNA levels in relation to cytological events during wild-type meiosis. *Above* Northern blots of mRNA isolated at the indicated time-points were hybridized with a *dmc1*-specific probe (*top row*) and a *rad51*-specific probe (*middle row*). *byr1* was used as a loading control (*bottom row*), as its expression does not change during meiosis (Nadin-Davis and Nasim 1990). *Below* Timing of cytological events during wild-type meiosis. Nuclei were visualized with the DNA-specific dye 4′,6-diamidino-2-phenylindole (DAPI). Cells with more than one nucleus have undergone the first meiotic division. The peak of cells containing more than one nucleus 1 h after induction is due to the last mitotic division before entry into meiosis from the G_1 phase (Bahler et al. 1998)

Deletion of *dmc1* does not affect *rad24* function

It was shown by Fukushima et al. (2000) that the *dmc1* gene is located immediately upstream of the *rad24* gene and that *dmc1*$^+$ and *rad24*$^+$ are co-transcribed during meiosis as a bicistronic RNA of 2.8 kb (Fig. 3). In addition, *rad24*$^+$ is transcribed as a 1-kb mRNA species during meiosis and mitosis. Rad24 is a 14-3-3 protein, required for DNA damage-checkpoint regulation (Ford et al. 1994) and entry into meiosis (Sato et al. 2002). Fukushima et al. (2000) constructed a *dmc1* disruption by inserting the *ura4*$^+$ gene into the middle of *dmc1*$^+$ (Fig. 3) and observed a reduction in meiotic recombination in the resulting strain. It is possible that the defect in meiotic recombination is due to interference with meiosis-specific co-expression of *rad24*$^+$ (abolition of bicistronic RNA).

To address this issue, we measured intragenic recombination between *lys7-1* and *lys7-2* in crosses homozygous for the *dmc1* deletion, but with ectopic expression of *dmc1*$^+$ at the *leu1* locus. The prototroph frequency in the *dmc1::ura4*$^+$ crosses was reduced four times (AG53×AG56; Fig. 4), while in cells expressing

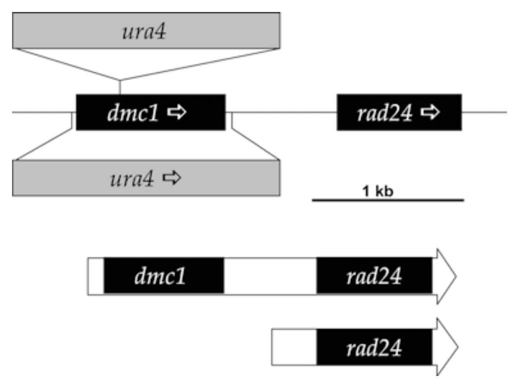

Fig. 3 Schematic diagram of the *dmc1-rad24* region, the disruptions of the *dmc1*$^+$ gene and the mRNA species. The *dmc1*$^+$ and *rad24*$^+$ ORFs are *indicated as black boxes* (Fukushima et al. 2000). *Arrows* indicate the direction of translation. *The shaded boxes* represent the *ura4*$^+$ marker gene. *Below* are two of the RNA species transcribed from the *dmc1-rad24* region, as determined by Fukushima et al. (2000)

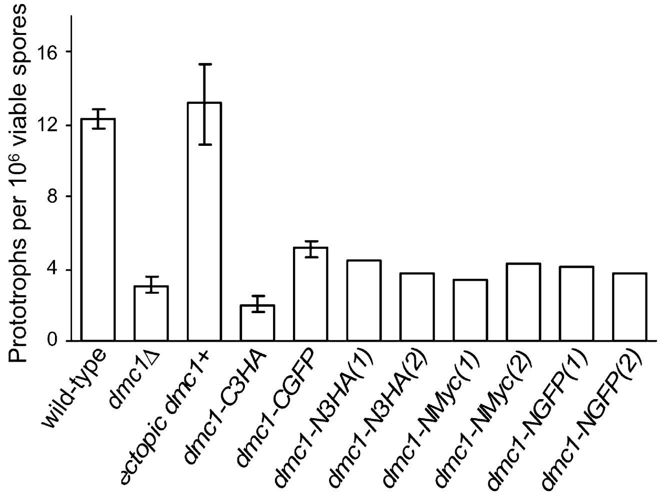

Fig. 4 Meiotic intragenic recombination frequency at *lys7* in *dmc1*$^{+}$-, *dmc1*Δ- and *dmc1*-tagged strains. Standard errors were determined (*error bars*) for crosses repeated at least three times

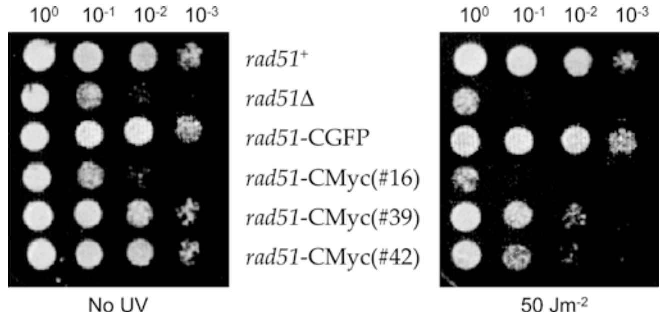

Fig. 5 UV-sensitivity of strains with C-terminally tagged *rad51*$^{+}$. *The scale above* indicates the dilution of the initial cultures. The following strains were used: 1-25 (*rad51*$^{+}$), AG69 (*rad51*Δ), AG484 (*rad51*-CGFP) and AG485 strains 16, 39 and 42 (*rad51*-CMyc; shown as *#16*, *#39*, *#42*, respectively)

ectopic *dmc1*$^{+}$ (AG104×AG105) it was not different from the wild type (3-106×4-150). Thus, the reduction in recombination frequency in the *dmc1::ura4*$^{+}$ strain is due to a loss of *dmc1*$^{+}$ function and not due to disturbance of *rad24*$^{+}$ function.

Fusion of epitope tags to *dmc1*$^{+}$ and *rad51*$^{+}$ results in loss of Dmc1 and Rad51 function

To study the subcellular localization of Dmc1 and Rad51 during meiosis, we tagged the genes at their endogenous loci. At the C-termini, the tags 3HA, 13Myc and GFP were introduced by the method described by Bahler et al. (1998). Stable transformants were checked by PCR for identification of those with homologous integration at the target locus. In the case of *rad51*, only normal-sized colonies were checked, since slow growth indicates loss of *rad51* function. The frequency of homologous integration was generally low (Table 4). In two cases, we did not identify any homologous integrants.

Disruption of *rad51* leads to slow growth and increased UV-sensitivity of the cells. Therefore normally growing G418-resistant transformants were selected and assayed for UV-sensitivity. The single *rad51*-CGFP isolate (AG484) was as resistant to UV as the wild type, while the three *rad51*-C13Myc strains (AG485) were UV-sensitive to different extents (Fig. 5). To show that the UV-sensitivity of these strains was due to the tagging and not caused by additional mutations elsewhere in the genome, we crossed the *rad51*-C13Myc strains against the wild type. All tested progeny strains with tags remained sensitive to UV (data not shown).

The *rad51*-CGFP strain and the least UV-sensitive of the three *rad51*-C13Myc strains (39) were further analyzed by sequencing. The epitope sequences of both tagged strains were defective. The GFP epitope tag in the *rad51*-CGFP strain contained a point mutation leading to the formation of a termination codon after the first nine amino acids of the epitope. The sequence of the 13Myc epitope tag in the *rad51*-C13Myc strain contained a deletion of 117 amino acids in the total of 177 residues. Thus, it is likely that strains with intact epitopes at the C-terminus of *rad51* acquire slow growth and UV-sensitivity. Transformants having no or only moderate defects had truncated tags.

An analogous analysis showed that integration of tagging fragments at the C-terminus of *dmc1*$^{+}$ was precise. No mutations were detected at the junctions between the chromosomal and inserted DNA or in the *dmc1*$^{+}$ sequence between the junction and the tag. Single-site insertion into the genome was checked by tetrad analysis. Viability of spores from *dmc1*-C3HA homozygous crosses was not affected, but the frequency of meiotic recombination was reduced in *dmc1*-C3HA and *dmc1*-CGFP strains (Fig. 4; data not shown). This indicates that fusion of 3HA or GFP epitopes to the C-terminus of the *dmc1*$^{+}$ gene results in loss of *dmc1*$^{+}$ function.

N-terminal epitope tagging of *dmc1*$^{+}$ was then performed. To retain *dmc1*$^{+}$ expression from its endogenous locus under regulation of its own promoter, we constructed a set of plasmids with a fragment of *Sch. pombe* genomic DNA containing any one of the three different tags 3HA, 13Myc or GFP, introduced right

Table 4 Efficiency of homologous integration of gene-targeting fragments for C-terminal tagging of the *dmc1*$^{+}$ and *rad51*$^{+}$ genes. For *rad51*$^{+}$, homologous integration is likely to be underestimated (see Results)

Gene	C-terminal tag	Total number of transformants checked by PCR	Homologous integration	Efficiency (%)
dmc1^{+}	3HA	14	3	21
	13Myc	60	0	0 ($<$1.7)
	GFP	28	1	3.6
rad51^{+}	3HA	152	0	0 ($<$0.7)
	13Myc	31	3	10
	GFP	7	1	14

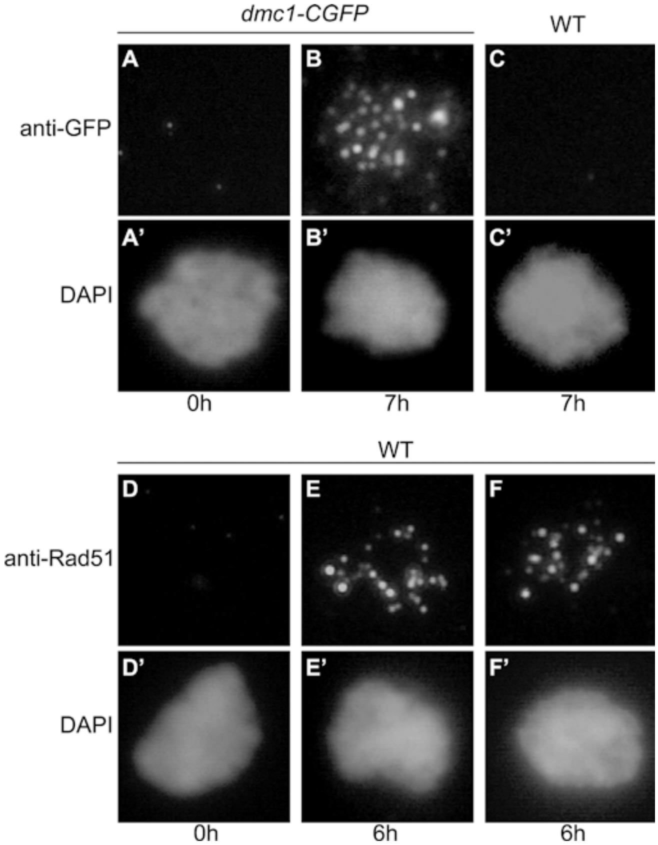

Fig. 6A–F Immunolocalization of Dmc1 and Rad51 on meiotic nuclear spreads. The spreads were prepared at the indicated time-points after the induction of meiosis. They were stained with DAPI (**A′**–**F′**) and immunostained with antibodies against GFP (**A**, **B**, **C**), human Rad51 (**D**, **E**) or *Sac. cerevisiae* Rad51 (**F**)

after the translation initiation codon of the *dmc1*$^{+}$ ORF (see Materials and methods). Single-site integration into the genome was checked by tetrad analysis. Meiotic recombination in the tagged strains was reduced to the level of *dmc1*Δ (Fig. 4). This indicates that fusion of 3HA, 13Myc or GFP epitopes to the N-terminus of the *dmc1*$^{+}$ gene results in loss of *dmc1*$^{+}$ function.

Immunolocalization of Dmc1 and Rad51 on spreads of meiotic chromatin

The Dmc1-CGFP or Dmc1-C3HA proteins localized as distinct foci on spreads from diploids homozygous for *dmc1*-CGFP (Fig. 6B) or *dmc1*-C3HA (data not shown) treated with anti-GFP or anti-HA antibody, respectively. Spread nuclei were prepared from diploid cells (D2 or D3) undergoing synchronous meiosis. The abundance of nuclei with foci (15–20%) was observed after initiation of meiosis and before the meiotic divisions (at 6–8 h after shifting to sporulation media). No staining was observed on spreads prepared from *dmc1*-CGFP and *dmc1*-C3HA cells at 0 h (induction of meiosis) or on spreads prepared from the wild-type diploid (D1) at any time (Fig. 6A, C; data not shown).

To study the localization of Rad51 during meiosis, we stained the nuclear spreads from wild-type diploids (D1) with a cross-reacting anti-human Rad51 antibody. We detected distinct foci (Fig. 6E) that mostly localized over the spread chromatin. The foci were observed in four independent time-courses (data not shown). No foci were observed on spreads prepared at the shift of cells to sporulation medium (Fig. 6D). We also stained meiotic nuclear spreads from the wild-type diploid with a cross-reacting anti-*Sac. cerevisiae* Rad51 antibody (a kind gift from A. Shinohara) and observed foci similar to those observed with anti-human Rad51 antibody (Fig. 6F).

Discussion

In this study, we further investigated the functions of *rad51*$^{+}$ and *dmc1*$^{+}$ of *Sch. pombe*. For this purpose we constructed full-gene deletions and epitope-tagged alleles.

The many roles of Rad51 in genome maintenance, recombination, vegetative growth and sporulation

Deletion of the *rad51*$^{+}$ gene conferred pronounced sensitivity to the DNA damaging agents UV and MMS, consistent with previously published observations on an insertion mutant (Muris et al. 1993). Jang et al. (1995) reported slow growth, aberrant morphology and elongation of cells of a *rad51* disruption mutant. We further investigated the slow-growth phenotype in *rad51::his3* deletion cells by pedigree analysis (Table 2). We showed that viable *rad51*Δ cells divided more slowly and that they were dying more frequently than wild-type cells. This indicates that the slow-growth phenotype of the *rad51*Δ mutant is caused by a viability decrease combined with an elongation of the cell cycle. The ratio between the doubling times of *rad51*Δ and the wild type was ~2, which is consistent with the observation of Jang et al. (1995). We also analyzed cells that, along with the *rad51* deletion, harbored the *mat1P*Δ*17::LEU2* mutation that abolishes DSB formation at the *mat1* locus; and we showed that *rad51*$^{+}$ is likely to play a role in repair of this DSB, as *rad51*Δ cells without the DSB die less frequently than those with the DSB (Table 2).

Mutations of the recombinational repair genes *rad22A*$^{+}$, *rhp54*$^{+}$ and *rhp55*$^{+}$ also lead to formation of elongated cells, aberrant morphology and impaired DNA content (Muris et al. 1996; Khasanov et al. 1999; Segurado et al. 2002). For the *rhp55* mutant, these phenotypes are also observed in the absence of a DSB at the *mat1* locus. Deletion of the *rad50* gene results in slower cell-doubling and an increase in death rate (Hartsuiker et al. 2001). Both phenotypes are reduced in the *smt0* cells. *rad50*, *rad51* and *rhp54* lose minichromosomes at elevated frequencies (Muris et al. 1996; Hartsuiker et al. 2001) and *rad22A* accumulates aberrant replication intermediates (Segurado et al. 2002). The observed phenotypes are consistent with these genes playing a role in genome stability in *Sch. pombe* through their involvement in DNA replication and, possibly, chromosome segregation. The defects are likely to lead to checkpoint-activated mitotic cell cycle delay (for discussion, see Jang et al. 1995; Muris et al. 1996). Similar effects of *rad50*, *rad51* and *rhp54* mutation on growth rate in budding yeast have not been reported. Only inactivation of the *RAD52* gene (homologue of *rad22A*) leads to slow growth in *Sac. cerevisiae* (Mortimer et al. 1981). In higher organisms, deletion of *RAD51* is lethal (Lim and Hasty 1996; Tsuzuki et al. 1996). Thus, the slow-growth phenotype of recombinational repair mutants in *Sch. pombe* makes them attractive models for understanding the causes of cell death in mammalian cells defective in the corresponding genes.

We showed that $rad51^+$ is required for mating-type switching. *rad51* can be assigned to class II *swi* mutants (Egel et al. 1984), because the h^{90} *rad51*Δ strain yielded both mottled and heterothallic colonies upon restreaking. About two-thirds of the heterothallic colonies were h^-. This is different from other class II mutants, where nearly all heterothallic segregants are h^+. However, there is another class II mutant known, *rad22A*, which segregates h^- heterothallic colonies (Ostermann et al. 1993). The observations made by us and other groups using the *smt0* and *mat1P*Δ*17::LEU2* mutations confirm the role of these genes in general genome stability, aside from repair of the DSB at the *mat1* locus leading to mating-type switching.

We showed that the efficiency of mating in crosses of heterothallic cells was reduced in *rad51*, *rhp55* and *rhp57* mutants (Table 3). This phenotype may be the consequence of the same DNA lesions occurring in vegetatively growing cells and leading to slow growth.

The observed instability of *rad51*Δ diploids is probably due to chromosome loss during propagation. Most aneuploid cells of *Sch. pombe* are not able to form colonies (Molnar et al. 1995). This probably contributed to the slower growth of the *rad51*Δ diploids in comparison with wild-type diploids and *rad51*Δ haploids. Almost no asci were observed after induction of meiosis. Difficulties with obtaining and propagating homozygous diploids were observed also in the *rad50*, *rhp54* and *rhp55* mutants of *Sch. pombe* (E. Hartsuiker, M. Catlett, S. L. Forsburg, F. Khasanov, personal communication). This suggests that proteins involved in homologous recombination are also important for the maintenance of the diploid state in *Sch. pombe* through their requirement for chromosome stability (Muris et al. 1996; Hartsuiker et al. 2001).

The intergenic meiotic recombination frequency in *rad51*Δ was reduced 2.3-fold compared with the wild type, consistent with the observation of Muris et al. (1997) for another interval and our results reported elsewhere (Grishchuk and Kohli 2003). Reduction in crossovers usually leads to a reduction in gamete viability (Baker et al. 1976). The low spore viability in *rad51*Δ crosses cannot be explained by a reduction in chiasmata only. The calculated average number of crossovers in meiosis of fission yeast is approximately 45 (Munz 1994). Taking into account that *Sch. pombe* has only three chromosomes, a 2-fold reduction in crossovers would still allow several chiasmata per chromosome pair and therefore cannot lead to the dramatic decrease in spore viability observed in the *rad51*Δ mutant (Table 3; Grishchuk and Kohli 2003). We suggest that the high spore lethality is caused by unrepaired DNA lesions, such as breaks and stalled replication forks arising before or after the induction of meiosis (see also Grishchuk and Kohli 2003). The spore viability reported in Table 2 is similar to the result (~8%) of Khasanov et al. (1999), who also used strains carrying small deletions at *mat1* preventing the DSB required for switching. Muris et al. (1997) reported ~2% spore viability in crosses in which only one of the parental strains contained the DSB preventing *smt0* mutation. This value is in the range of spore viability in crosses carrying wild-type *mat1* loci on both chromosomes (~3%; Grishchuk and Kohli 2003). Thus, the major contribution of Rad51-mediated repair concerns general genome stability. Repair of the DSB at *mat1* by Rad51 yields a minor contribution to spore viability.

The role of Dmc1 in meiosis

In contrast to *rad51*Δ, *dmc1*Δ did not show any defects during vegetative growth. Direct evidence for the involvement of Dmc1 in meiotic recombination is the reduction in recombination frequencies detected in *dmc1*Δ cells (Fig. 4). Our results are comparable with those reported by Fukushima et al. (2000) for an incomplete $dmc1^+$ disruption. Elsewhere, we reported that Dmc1 is (besides Rad51) the major recombination protein in meiosis of fission yeast, while the three other RecA paralogues (Rhp55, Rhp57, Rlp1) play accessory roles. But with respect to spore viability, *dmc1*Δ hardly differs from the wild type (Grishchuk and Kohli 2003).

The expression of Rad51 and Dmc1 during meiosis

We observed multiple bands with the *rad51*-specific probe. There are three other genes with homology to *recA* in *Sch. pombe* that also have ORF sizes similar to $rad51^+$: $rhp55^+$, $rhp57^+$ and $rlp1^+$. The probe used to detect *rad51* mRNA was derived from the 5′ end of the gene, where the homology among *recA*-like genes is lowest. The homology search with this probe against the *Sch. pombe* genome did not reveal any significant matches besides *rad51*. With this probe, we did not detect *dmc1* mRNA, which is larger than the *rad51* mRNA and presumably also larger than other *recA*-like genes (data not shown). Taking these observations together, we think that cross-hybridization of the *rad51*-derived probe with transcripts of other *recA* genes is quite unlikely. We could not test the cross-reactivity of our probe during meiosis, since *rad51*Δ diploids were unstable.

Our observation that *rad51* and *dmc1* mRNAs are present during meiosis (Fig. 2) is consistent with the proposed involvement of Rad51 and Dmc1 in meiotic events. We determined that the highest transcription of *dmc1*$^{+}$ and *rad51*$^{+}$ occurred when most of the cells were undergoing meiotic prophase. This is in agreement with Fukushima et al. (2000), who used Northern analysis to detect increased levels of *dmc1*$^{+}$ transcription several hours after the induction of meiosis, and with the results of Mata et al. (2002), who showed in a microarray experiment that the transcription of *rad51*$^{+}$ and *dmc1*$^{+}$ is significantly induced during meiotic prophase. The amounts of *rad51*$^{+}$ and *dmc1*$^{+}$ mRNAs are higher compared with other *recA*-like genes (J. Mata, personal communication), consistent with our proposal that Rad51 and Dmc1 play major roles in meiotic recombination, while Rhp55, Rhp57 and Rlp1 play accessory roles. The expression of *dmc1*$^{+}$ is much lower than that of *rad51*$^{+}$ during vegetative growth. It dramatically increases during prophase and later decreases. This is consistent with *dmc1*$^{+}$ being involved in meiotic recombination, but lacking a role in general DNA damage repair and, as a consequence, promoting high spore viability. The co-transcription of *dmc1*$^{+}$ with the downstream *rad24*$^{+}$ gene is unusual for eukaryotic cells (Fukushima et al. 2000). But we showed that the reduction in recombination frequency in the *dmc1* deletion strains is not due to the disturbance of *rad24*$^{+}$ expression (Fig. 4).

The localization of Rad51 and Dmc1 proteins in meiotic nuclei

With cross-reacting anti-human Rad51 antibody and anti-*Sac. cerevisiae* Rad51 antibody, we observed foci on spread chromatin of cells undergoing meiosis (Fig. 6). It was not possible to test whether the anti-Rad51 antibodies cross-reacted with other proteins on meiotic chromatin, since the *rad51*Δ diploids were unstable. Although definitive proof is missing, the cross-reactivity of anti-human Rad51 antibody with *Sch. pombe* Dmc1 is highly improbable, since the sequence similarity between the N-terminus of hRad51 used as an antigene to raise the antibody and the *Sch. pombe* Dmc1 protein is very low (46%). In addition, evidence for the specific recognition of *Sch. pombe* Rad51 by anti-human Rad51 antibody in mitotic cells was published by Caspari et al. (2002). In a preliminary quantitation experiment, up to 30 foci were observed per meiotic nucleus, with an average of 13 ± 7 at 5–6 h after induction of meiosis (data not shown).

Dmc1-CGFP and Dmc1-C3HA were found to form foci on spread chromatin of cells undergoing meiosis (Fig. 6). Since the tagged proteins cannot fulfill the wild-type function (Fig. 4), it is difficult to decide whether the observed foci represent the natural location of Dmc1. However, an abundance of foci was observed only after the initiation of meiosis and before the meiotic divisions. Thus, their appearance coincided with the time of action of Dmc1 in meiotic recombination. In a preliminary quantitation experiment, up to 75 foci were observed per meiotic nucleus, with an average of 35 ± 18 at 4–6 h after induction of meiosis (data not shown). As for Rad51 foci, the conditions were not optimized and the experiments not repeated. Thus, we refrain from speculating on the relation between foci and crossover numbers [on average 45 per meiosis, as reported by Munz (1994)].

We made several attempts to obtain strains expressing functional Dmc1 and Rad51 proteins carrying epitope tags suitable for cytology. Strains with *dmc1* carrying N- and C-terminal tags all showed the *dmc1*Δ phenotype (Fig. 4). In the case of C-terminal tagging of *rad51*, we obtained transformants that were moderately sensitive to UV and carried truncated tags. One UV-resistant transformant carried only the codons for the first nine amino acids of the GFP tag. Some transformants displayed the slow-growth phenotype of *rad51*Δ strains (data not shown). These transformants may have carried full-length epitopes, but were not further analyzed. We conclude that tagging the Dmc1 and Rad51 proteins of *Sch. pombe* in the ways attempted leads to loss of function. In contrast, Dresser et al. (1997) reported functional HA-tagging at the C-terminus of *Sac. cerevisiae* Dmc1, but did not present data on meiotic recombination frequencies in this strain background. RecA is able to form a nucleoprotein filament, within which the DNA interaction takes place during strand transfer. Purified *Sac. cerevisiae* and human Rad51 proteins bind DNA to form helical nucleoprotein filaments (Ogawa et al. 1993; Benson et al. 1994). Human Dmc1 protein in vitro forms octameric rings on the DNA (Passy et al. 1999). Homotypic interactions involving the ends of Rad51 and Dmc1 proteins may be indispensable for proper function. In addition, Rad51 of *Sch. pombe* and other organisms was shown to interact with a number of other proteins (Donovan et al. 1994; Hays et al. 1995; Johnson and Symington 1995; Clever et al. 1997; Tsutsui et al. 2001). Fusion of epitope tags to the N- or C-terminus of Rad51 and Dmc1 proteins may prevent the binding of these other proteins. Nevertheless, the obtained epitope constructions will be useful for future experiments.

In conclusion, the analysis of full-gene deletions and epitope-tagging of *rad51* and *dmc1* of *Sch. pombe* lead to novel insights into their roles in normal cell cycle progression and meiosis.

Acknowledgements We thank A. Shinohara for plasmids prad51 and pdmc1 and for the anti-*Sac. cerevisiae* Rad51 antibody, P. Silver for the antibody against GFP, A.M. Schweingruber for the *byr1* probe and M. Catlett, S.L. Forsburg, E. Hartsuiker, F. Khasanov and J. Mata for their communication of unpublished data. We are grateful to E. Grishchuk for helpful discussions throughout this work and to G.R. Smith for comments on the manuscript. This work was supported by grants from the Swiss National Science Foundation, by the SCOPES program of the Swiss Government and by a grant from the Human Frontiers Science Program.

References

Aboussekhra A, Chanet R, Adjiri A, Fabre F (1992) Semidominant suppressors of Srs2 helicase mutations of *Saccharomyces cerevisiae* map in the *RAD51* gene, whose sequence predicts a protein with similarities to procaryotic RecA proteins. Mol Cell Biol 12:3224–3234

Akaboshi E, Inoue Y, Ryo H (1994) Cloning of the cDNA and genomic DNA that correspond to the *recA*-like gene of *Drosophila melanogaster*. Jpn J Genet 69:663–670

Arcangioli B (1998) A site- and strand-specific DNA break confers asymmetric switching potential in fission yeast. EMBO J 17:4503–4510

Arcangioli B, Klar AJ (1991) A novel switch-activating site (*SAS1*) and its cognate binding factor (*SAP1*) required for efficient *mat1* switching in *Schizosaccharomyces pombe*. EMBO J 10:3025–3032

Arcangioli B, Lahondes R de (2000) Fission yeast switches mating type by a replication–recombination coupled process. EMBO J 19:1389–1396

Bahler J, et al (1998) Heterologous modules for efficient and versatile PCR-based gene targeting in *Schizosaccharomyces pombe*. Yeast 14:943–951

Baker BS, Carpenter AT, Esposito MS, Esposito RE, Sandler L (1976) The genetic control of meiosis. Annu Rev Genet 10:53–134

Barlow AL, Benson FE, West SC, Hulten MA (1997) Distribution of the Rad51 recombinase in human and mouse spermatocytes. EMBO J 16:5207–5215

Basile G, Aker M, Mortimer RK (1992) Nucleotide sequence and transcriptional regulation of the yeast recombinational repair gene *RAD51*. Mol Cell Biol 12:3235–3246

Baumann P, Benson FE, West SC (1996) Human Rad51 protein promotes ATP-dependent homologous pairing and strand transfer reactions in vitro. Cell 87:757–766

Beach DH, Klar AJ (1984) Rearrangements of the transposable mating-type cassettes of fission yeast. EMBO J 3:603–610

Beach D, Rodgers L, Gould J (1985) *ran1*+ controls the transition from mitotic division to meiosis in fission yeast. Curr Genet 10:297–311

Benson FE, Stasiak A, West SC (1994) Purification and characterization of the human Rad51 protein, an analogue of *E. coli* RecA. EMBO J 13:5764–5771

Bezzubova O, Shinohara A, Mueller RG, Ogawa H, Buerstedde JM (1993) A chicken *RAD51* homologue is expressed at high levels in lymphoid and reproductive organs. Nucleic Acids Res 21:1577–1580

Bishop DK (1994) RecA homologs Dmc1 and Rad51 interact to form multiple nuclear complexes prior to meiotic chromosome synapsis. Cell 79:1081–1092

Bishop DK, Park D, Xu L, Kleckner N (1992) DMC1: a meiosis-specific yeast homolog of *E. coli recA* required for recombination, synaptonemal complex formation, and cell cycle progression. Cell 69:439–456

Burke JD, Gould KL (1994) Molecular cloning and characterization of the *Schizosaccharomyces pombe his3* gene for use as a selectable marker. Mol Gen Genet 242:169–176

Caspari T, Murray JM, Carr AM (2002) Cdc2-cyclin B kinase activity links Crb2 and Rqh1-topoisomerase III. Genes Dev 16:1195–1208

Clever B, Interthal H, Schmuckli-Maurer J, King J, Sigrist M, Heyer WD (1997) Recombinational repair in yeast: functional interactions between Rad51 and Rad54 proteins. EMBO J 16:2535–2544

Couteau F, Belzile F, Horlow C, Grandjean O, Vezon D, Doutriaux MP (1999) Random chromosome segregation without meiotic arrest in both male and female meiocytes of a *dmc1* mutant of *Arabidopsis*. Plant Cell 11:1623–1634

Dalgaard JZ, Klar AJ (1999) Orientation of DNA replication establishes mating-type switching pattern in *S. pombe*. Nature 400:181–184

Donovan JW, Milne GT, Weaver DT (1994) Homotypic and heterotypic protein associations control Rad51 function in double-strand break repair. Genes Dev 8:2552–2562

Doutriaux MP, Couteau F, Bergounioux C, White C (1998) Isolation and characterisation of the *RAD51* and *DMC1* homologs from *Arabidopsis thaliana*. Mol Gen Genet 257:283–291

Dresser ME, et al (1997) DMC1 functions in a *Saccharomyces cerevisiae* meiotic pathway that is largely independent of the *RAD51* pathway. Genetics 147:533–544

Egel R, Beach DH, Klar AJ (1984) Genes required for initiation and resolution steps of mating-type switching in fission yeast. Proc Natl Acad Sci USA 81:3481–3485

Ford JC, al-Khodairy F, Fotou E, Sheldrick KS, Griffiths DJ, Carr AM (1994) 14-3-3 protein homologs required for the DNA damage checkpoint in fission yeast. Science 265:533–535

Fukushima K, et al (2000) Dmc1 of *Schizosaccharomyces pombe* plays a role in meiotic recombination. Nucleic Acids Res 28:2709–2716

Grimm C, Kohli J, Murray J, Maundrell K (1988) Genetic engineering of *Schizosaccharomyces pombe*: a system for gene disruption and replacement using the *ura4* gene as a selectable marker. Mol Gen Genet 215:81–86

Grimm C, Schaer P, Munz P, Kohli J (1991) The strong *ADH1* promoter stimulates mitotic and meiotic recombination at the *ADE6* gene of *Schizosaccharomyces pombe*. Mol Cell Biol 11:289–298

Grishchuk A, Kohli J (2003) Five RecA-like proteins of *Schizosaccharomyces pombe* are involved in meiotic recombination. Genetics (in press)

Gutz H, Heslot H, et al (1974) *Schizosaccharomyces pombe*. In: King RC (ed) Handbook of genetics. Plenum, New York

Hartsuiker E, Vaessen E, Carr AM, Kohli J (2001) Fission yeast Rad50 stimulates sister chromatid recombination and links cohesion with repair. EMBO J 20:6660–6671

Hays SL, Firmenich AA, Berg P (1995) Complex formation in yeast double-strand break repair: participation of Rad51, Rad52, Rad55, and Rad57 proteins. Proc Natl Acad Sci USA 92:6925–6929

Ito H, Fukuda Y, Murata K, Kimura A (1983) Transformation of intact yeast cells treated with alkali cations. J Bacteriol 153:163–168

Jang YK, Jin YH, Kim EM, Fabre F, Hong SH, Park SD (1994) Cloning and sequence analysis of *rhp51*+, a *Schizosaccharomyces pombe* homolog of the *Saccharomyces cerevisiae RAD51* gene. Gene 142:207–211

Jang YK, et al (1995) Evidences for possible involvement of Rhp51 protein in mitotic events including chromosome segregation. Biochem Mol Biol Int 37:329–337

Johnson RD, Symington LS (1995) Functional differences and interactions among the putative RecA homologs Rad51, Rad55, and Rad57. Mol Cell Biol 15:4843–4850

Keeney JB, Boeke JD (1994) Efficient targeted integration at leu1–32 and ura4–294 in *Schizosaccharomyces pombe*. Genetics 136:849–856

Khasanov FK, Savchenko GV, Bashkirova EV, Korolev VG, Heyer WD, Bashkirov VI (1999) A new recombinational DNA repair gene from *Schizosaccharomyces pombe* with homology to *Escherichia coli* RecA. Genetics 152:1557–1572

Kowalczykowski SC, Dixon DA, Eggleston AK, Lauder SD, Rehrauer WM (1994) Biochemistry of homologous recombination in *Escherichia coli*. Microbiol Rev 58:401–465

Leupold U (1955) Methodisches zur Genetic von *Schizosaccharomyces pombe*. Schweiz Z Allg Pathol Bakteriol 18:1141–1146

Lim DS, Hasty P (1996) A mutation in mouse *rad51* results in an early embryonic lethal that is suppressed by a mutation in *p53*. Mol Cell Biol 16:7133–7143

Masson JY, West SC (2001) The Rad51 and Dmc1 recombinases: a non-identical twin relationship. Trends Biochem Sci 26:131–136

Mata J, Lyne R, Burns G, Bahler J (2002) The transcriptional program of meiosis and sporulation in fission yeast. Nat Genet 32:143–147

Molnar M, Bahler J, Sipiczki M, Kohli J (1995) The *rec8* gene of *Schizosaccharomyces pombe* is involved in linear element formation, chromosome pairing and sister-chromatid cohesion during meiosis. Genetics 141:61–73

Mortimer RK, Contopoulou R, Schild D (1981) Mitotic chromosome loss in a radiation-sensitive strain of the yeast *Saccharomyces cerevisiae*. Proc Natl Acad Sci USA 78:5778–5782

Munz P (1994) An analysis of interference in the fission yeast *Schizosaccharomyces pombe*. Genetics 137:701–707

Muris DF, et al (1993) Cloning the *RAD51* homologue of *Schizosaccharomyces pombe*. Nucleic Acids Res 21:4586–4591

Muris DF, et al (1996) Isolation of the *Schizosaccharomyces pombe RAD54* homologue, *rhp54+*, a gene involved in the repair of radiation damage and replication fidelity. J Cell Sci 109:73–81

Muris DF, et al (1997) Homologous recombination in the fission yeast *Schizosaccharomyces pombe*: different requirements for the *rhp51+*, *rhp54+* and *rad22+* genes. Curr Genet 31:248–254

Nadin-Davis SA, Nasim A (1990) *Schizosaccharomyces pombe ras1* and *byr1* are functionally related genes of the *ste* family that affect starvation-induced transcription of mating-type genes. Mol Cell Biol 10:549–560

Ogawa T, Yu X, Shinohara A, Egelman EH (1993) Similarity of the yeast *RAD51* filament to the bacterial RecA filament. Science 259:1896–1899

Ostermann K, Lorentz A, Schmidt H (1993) The fission yeast *rad22* gene, having a function in mating-type switching and repair of DNA damages, encodes a protein homolog to Rad52 of *Saccharomyces cerevisiae*. Nucleic Acids Res 21:5940–5944

Parisi S, et al (1999) Rec8p, a meiotic recombination and sister chromatid cohesion phosphoprotein of the Rad21p family conserved from fission yeast to humans. Mol Cell Biol 19:3515–3528

Park SD, Jin YH, Jang YK (1998) Regulation of DNA damage inducible *rhp51+* gene, a *recA* homolog from *Schizosaccharomyces pombe*. J Toxicol Sci 23 [Suppl 2]:110–116

Passy SI, et al (1999) Human Dmc1 protein binds DNA as an octameric ring. Proc Natl Acad Sci USA 96:10684–10688

Pittman DL, et al (1998) Meiotic prophase arrest with failure of chromosome synapsis in mice deficient for Dmc1, a germline-specific RecA homolog. Mol Cell 1:697–705

Rockmill B, Sym M, Scherthan H, Roeder GS (1995) Roles for two RecA homologs in promoting meiotic chromosome synapsis. Genes Dev 9:2684–2695

Sato M, Watanabe Y, Akiyoshi Y, Yamamoto M (2002) 14-3-3 protein interferes with the binding of RNA to the phosphorylated form of fission yeast meiotic regulator Mei2p. Curr Biol 12:141–145

Seedorf M, Damelin M, Kahana J, Taura T, Silver PA (1999) Interactions between a nuclear transporter and a subset of nuclear pore complex proteins depend on Ran GTPase. Mol Cell Biol 19:1547–1557

Segurado M, Gomez M, Antequera F (2002) Increased recombination intermediates and homologous integration hot spots at DNA replication origins. Mol Cell 10:907–916

Shinohara A, Ogawa H, Ogawa T (1992) Rad51 protein involved in repair and recombination in *S. cerevisiae* is a RecA-like protein. Cell 69:457–470

Shinohara A, Ogawa H, Matsuda Y, Ushio N, Ikeo K, Ogawa T (1993) Cloning of human, mouse and fission yeast recombination genes homologous to *RAD51* and *recA*. Nat Genet 4:239–243

Shinohara A, Gasior S, Ogawa T, Kleckner N, Bishop DK (1997) *Saccharomyces cerevisiae recA* homologues *RAD51* and *DMC1* have both distinct and overlapping roles in meiotic recombination. Genes Cells 2:615–629

Shinohara M, Gasior SL, Bishop DK, Shinohara A (2000) Tid1/Rdh54 promotes colocalization of *rad51* and *dmc1* during meiotic recombination. Proc Natl Acad Sci USA 97:10814–10819

Smith GR, Amundsen SK, Dabert P, Taylor AF (1995) The initiation and control of homologous recombination in *Escherichia coli*. Philos Trans R Soc Lond B Biol Sci 347:13–20

Story RM, Bishop DK, Kleckner N, Steitz TA (1993) Structural relationship of bacterial RecA proteins to recombination proteins from bacteriophage T4 and yeast. Science 259:1892–1896

Styrkarsdottir U, Egel R, Nielsen O (1993) The *smt-0* mutation which abolishes mating-type switching in fission yeast is a deletion. Curr Genet 23:184–186

Sung P (1994) Catalysis of ATP-dependent homologous DNA pairing and strand exchange by yeast RAD51 protein. Science 265:1241–1243

Tsutsui Y, Morishita T, Iwasaki H, Toh H, Shinagawa H (2000) A recombination repair gene of *Schizosaccharomyces pombe*, *rhp57*, is a functional homolog of the *Saccharomyces cerevisiae RAD57* gene and is phylogenetically related to the human *XRCC3* gene. Genetics 154:1451–1461

Tsutsui Y, Khasanov FK, Shinagawa H, Iwasaki H, Bashkirov VI (2001) Multiple interactions among the components of the recombinational DNA repair system in *Schizosaccharomyces pombe*. Genetics 159:91–105

Tsuzuki T, et al (1996) Targeted disruption of the Rad51 gene leads to lethality in embryonic mice. Proc Natl Acad Sci USA 93:6236–6240

Watanabe Y, Lino Y, Furuhata K, Shimoda C, Yamamoto M (1988) The *S. pombe mei2* gene encoding a crucial molecule for commitment to meiosis is under the regulation of cAMP. EMBO J 7:761–767